





Hydro-Meteorological Drivers of Event Runoff Characteristics Under Analogous Soil Moisture Patterns in Three Small-Scale Headwater Catchments

¹BOKU University, Institute of Soil Physics and Rural Water Management, Department of Landscape, Water and Infrastructure, Vienna,

Austria | ²Forschungszentrum Jülich GmbH, Institute of Bio-and Geosciences, Agrosphere Institute (IBG-3), Wilhelm-Johnen-Straße, Jülich,

Germany | ³Institute for Land and Water Management Research, Federal Agency for Water Management, Petzenkirchen, Austria | ⁴Institute of Hydraulic

Engineering and Water Resources Management, Vienna University of Technology, Vienna, Austria

Correspondence: Adriane Hövel (adriane.hoevel@boku.ac.at)

Received: 16 October 2024 | Revised: 22 April 2025 | Accepted: 22 May 2025

Funding: This work was supported by the Austrian Science Fund (10.55776/P34666) with additional support from the BOKU University, Vienna. The work of Adriane Hövel was supported by the Doctoral School 'Human River Systems in the 21st Century (HR21)' of the BOKU University, Vienna.

 $\textbf{Keywords:} \ catchment \ hydrology \ | \ patterns \ | \ rainfall-runoff \ | \ runoff \ characteristics \ | \ soil \ moisture \ | \ thresholds$

ABSTRACT

A catchment's runoff response to precipitation largely depends on the antecedent soil moisture and on the characteristics of the precipitation event, but also on other hydro-meteorological conditions, such as evapotranspiration. Studies investigating the effects of hydro-meteorological variables on runoff characteristics in catchments with daily temporal resolution mostly used surrogate measures of soil moisture derived from hydrological models or remote sensing products. Here, we applied a time series-based pattern search to up to 12 years of daily in situ measured soil moisture in three depths (5, 20 and 50 cm) in three headwater catchments, two of which are located in Germany (forest and grassland) and one in Austria (agriculture), to identify key variables influencing runoff characteristics under analogous soil moisture patterns. After detecting groups of analogous soil moisture, we split the corresponding runoff into similar and different patterns based on goodness-of-fit criteria and analysed their influencing hydro-meteorological variables with descriptive statistics and Spearman rank correlation coefficients (ρ). Results showed that in the forest and in the grassland catchment, the antecedent soil moisture mainly influenced runoff characteristics for analogous soil moisture patterns. In the agricultural catchment in Austria, both the antecedent soil moisture and rainfall characteristics had an influence on runoff characteristics. The proposed method can be used to evaluate hydro-meteorological drivers of event runoff characteristics under analogous soil moisture. In this way, hydrological processes that dominate in either group of similar or different runoff patterns can be differentiated, providing insights into the potential predictability of the respective runoff pattern.

1 | Introduction

The runoff response to a rainfall event at the catchment scale is driven by hydro-climatic and physical catchment characteristics (Chen et al. 2020a, 2020b; Jencso and McGlynn 2011). It

is the most comprehensive signature of catchment behaviour since it integrates information about different runoff generation processes (Blöschl et al. 2013). Event runoff responses are spatiotemporally variable as they depend on antecedent soil moisture (ASM) (e.g., Penna et al. 2011; Saffarpour et al. 2016),

This is an open access article under the terms of the Creative Commons Attribution License, which permits use, distribution and reproduction in any medium, provided the original work is properly cited.

© 2025 The Author(s). Hydrological Processes published by John Wiley & Sons Ltd.

rainfall characteristics (Blume et al. 2007), and other hydrometeorological drivers, for example, evapotranspiration (Guo et al. 2017a; Rossi et al. 2016). Previous studies evaluated runoff generation mechanisms (e.g., Gaál et al. 2012, 2015; Stein et al. 2020; Tarasova, Basso, Poncelet, et al. 2018), runoff prediction in ungauged basins (e.g., Parajka et al. 2007) and nutrient transport processes (Grimaldi et al. 2009; James and Roulet 2007). Thus, exploring drivers of event runoff characteristics contributes to the understanding of catchment-scale hydrological processes and is crucial for informed decisionmaking in water resources management and hydrological modelling (Hrachowitz et al. 2013). Furthermore, the assessment of hydrological processes at the catchment scale is of significant importance for the development of measurement strategies and their validation (Brocca et al. 2012; Mohanty et al. 2017).

However, studies assessing the spatiotemporal dynamics of runoff responses and the factors that drive the fast mobilisation of water stored in the catchment for a long time still remain scarce (Kirchner 2024). Although runoff dynamics were evaluated in single (e.g., Guo et al. 2017b) and multiple catchments with sizes ranging from approx. 5 to 20000 km² (Gaál et al. 2012; Merz and Blöschl 2009; Tarasova, Basso, Zink, et al. 2018; Zheng et al. 2023), only some of them analysed runoff events based on a large sample of events (e.g., Ali et al. 2010; Tarasova, Basso, Zink, et al. 2018). At the event scale, climatic variables, including potential evapotranspiration (PET) and the aridity index, were found to be negatively correlated with the event runoff coefficient (ERC) (ratio of runoff-to-precipitation), highlighting the role of PET in mediating the long-term water storage in soils (Merz and Blöschl 2009; Rossi et al. 2016; Tarasova, Basso, Zink, et al. 2018; Zheng et al. 2023). Furthermore, ERC was positively correlated with the mean annual precipitation in catchments across Austria (Merz et al. 2006; Merz and Blöschl 2009) and with event rainfall volumes in large-scale catchments in Germany that had limited storage capacity (Tarasova, Basso, Poncelet, et al. 2018). On the contrary, Zheng et al. (2023) found a weak correlation between rainfall volumes and ERC in catchments with large storage capacity.

Besides the solely rainfall-derived variables, event runoff variability at the daily scale may be linked to the mean annual or seasonal partitioning of precipitation into evapotranspiration and runoff via soil moisture dynamics (Latron and Gallart 2008; Rossi et al. 2016). In Austria (Merz and Blöschl 2009) and the United Kingdom (Zheng et al. 2023), ERC and soil moisture followed the same seasonality. In this regard, ASM has been shown to strongly influence catchmentscale runoff characteristics (e.g., Penna et al. 2011; Saffarpour et al. 2016). A nonlinear threshold behaviour of the runoff response has frequently been observed in catchments where runoff significantly increased after a certain soil moisture threshold was exceeded (Detty and McGuire 2010; Jencso et al. 2009; Penna et al. 2011; Stockinger et al. 2014). In particular, the threshold behaviour was apparent in catchments with a humid climate and forest cover (e.g., Detty and McGuire 2010; Vichta et al. 2024), but also in catchments with other land use types such as alpine grassland (Penna et al. 2011) or intensively grazed pasture (Saffarpour et al. 2016).

Despite these advancements, relatively few studies used soil moisture observations at a high spatiotemporal resolution over a long time span to characterise the rainfall-runoff process at the catchment scale (Singh et al. 2021; Vichta et al. 2024). Mostly, substitute measures were used, for example, soil moisture derived from hydrological models or remote sensing products, without discretisation of different depths (e.g., Yao et al. 2020; Zheng et al. 2023). Therefore, a better representation of soil moisture is necessary to quantify key influencing variables on the runoff response (Rossi et al. 2016). Furthermore, the few field-based studies investigating rainfall-runoff processes using in situ measured soil moisture were focused on forested catchments and mainly conducted at one site only (e.g., Vichta et al. 2024). However, the investigation of runoff generation mechanisms in small-scale catchments with different land use types offers the opportunity to assess the impact of different land use types on rainfall-runoff processes. For example, by clustering similar runoff responses, Hövel et al. (2024a) found that the respective temporal pattern of soil moisture was an important indicator of similar runoff responses in two small-scale catchments with differing land use types of forest and grassland. However, they did not investigate temporal patterns in the entire soil moisture time series itself, that is, independent of the times of runoff responses. Examining temporal patterns in both runoff and soil moisture at the same time could help to comprehensively understand catchment-scale rainfall-runoff processes (Blöschl 2006).

In this study, we addressed this gap by using repeating temporal patterns in soil moisture and runoff at the catchment scale to investigate the interaction between hydro-meteorological variables and event runoff characteristics. To do this, we adopted the approach suggested by Hövel et al. (2024a), but instead of clustering similar runoff responses, we searched for soil moisture patterns averaged over the catchment area in three small-scale catchments with different land use types of forest, grassland and agriculture. In each catchment, we used high-resolution in situ soil moisture observations for the pattern search. For each group of analogous soil moisture, we divided the respective runoff into similar and different patterns by means of goodness-of-fit criteria to investigate event runoff characteristics and their drivers separately. Therefore, the objectives of the present study were to (1) detect repeating temporal patterns of in situ soil moisture observations, (2) compare the characteristics of similar and different runoff patterns in terms of their major hydro-meteorological drivers and (3) assess the impact of hydro-meteorological variables on runoff characteristics under analogous soil moisture identified in the first objective.

2 | Study Area and Data

2.1 | Study Sites

Based on their spatiotemporally high-resolution data, we selected three small-scale catchments in Germany and Austria (Figure 1). The forest (38.5 ha, Wüstebach) and grassland (40 ha, Rollesbroich) headwater catchments are located in the Eifel region of western Germany and belong to the Terrestrial Environmental Observatories network (TERENO) (Bogena

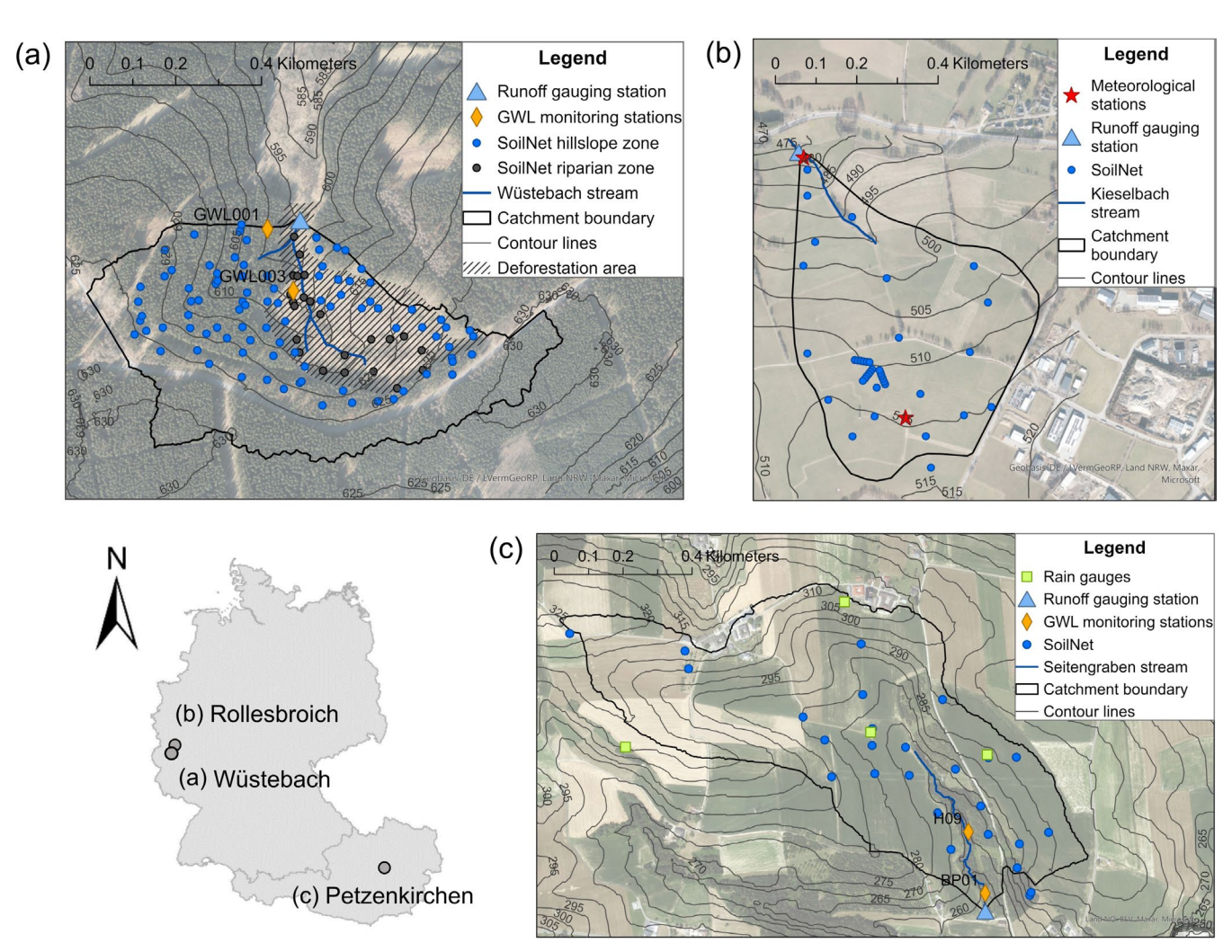


FIGURE 1 | Location and land use maps of the three study catchments in Germany and Austria indicating measurement sites with (a) Wüstebach (partly deforested in 2013), (b) Rollesbroich (extensively managed grassland) and (c) Petzenkirchen (agriculture) (Hövel et al. 2024a).

et al. 2018). Due to their proximity, they are characterised by a similar climate, with a mean annual precipitation of about 1224 and 970 mm yr⁻¹, mean annual temperature of 8.0°C and 8.1°C and mean annual discharge of about 734 and 529 mm yr⁻¹ (2008– 2021) in the forest and grassland catchment, respectively. Soil types of Cambisol and Planosol are predominant in the hillslope zone of the forest catchment, while the riparian zone (10% of the catchment) is characterised by Gleysols and Histosols. Similarly, gleyic Cambisols prevail further upstream in the grassland catchment, while Stagnosols dominate closer to the outlet (Bogena et al. 2018). Soil depths in the two catchments range from less than 1 m up to a maximum of 2 and 1.5 m in the forest and grassland catchment, respectively (Gebler et al. 2019; Graf et al. 2014). In the forest catchment, periglacial layers cover the bedrock (Borchardt 2012), which consists of Devonian shales and sandstone (Richter 2008), while in the grassland, the bedrock is covered by weathered saprolite (Gebler et al. 2019). Mainly, the riparian zone (8 ha, 21% of the area) of the forest catchment was deforested in September 2013 (Bogena et al. 2018; Wiekenkamp et al. 2016a). After the clear-cutting, a natural reforestation took place. In the grassland catchment, a drainage system affecting fast runoff processes is in the source area (Gebler et al. 2019). The Hydrological Open Air Laboratory (HOAL) agricultural catchment (66 ha, Petzenkirchen) lies in the western part of Lower

Austria and has a mean annual precipitation, temperature and discharge of about $823\,\mathrm{mm\,yr^{-1}}$, $9.5^{\circ}\mathrm{C}$ and $195\,\mathrm{mm\,yr^{-1}}$ (1990-2014), respectively. The catchment has Gleysols in the riparian zone, while Cambisols and Planosols predominate in most other areas. Soils are shallow and characterised by medium to poor infiltration capacity, with the underlying bedrock consisting of tertiary sediments of the Molasse zone and fractured siltstone (Blöschl et al. 2016). Tile drains are installed in around 15% of the area, and 25% of the stream is piped, leading to complex, area-specific flow mechanisms (Vreugdenhil et al. 2022).

2.2 | Data

We used high-resolution data on precipitation, runoff, ground-water levels and in situ soil moisture measurements in 5, 20 and 50 cm depth. Details on the number of measurement locations for each variable and their spatial distribution are given in the following subsections. Figure 2 displays the data for the forest catchment, while the data for the grassland and agricultural catchments are shown in Supporting Information S1. A detailed description of the data pre-processing and quality control can be found in sect. 3 'Data and methods' in Hövel et al. (2024a).

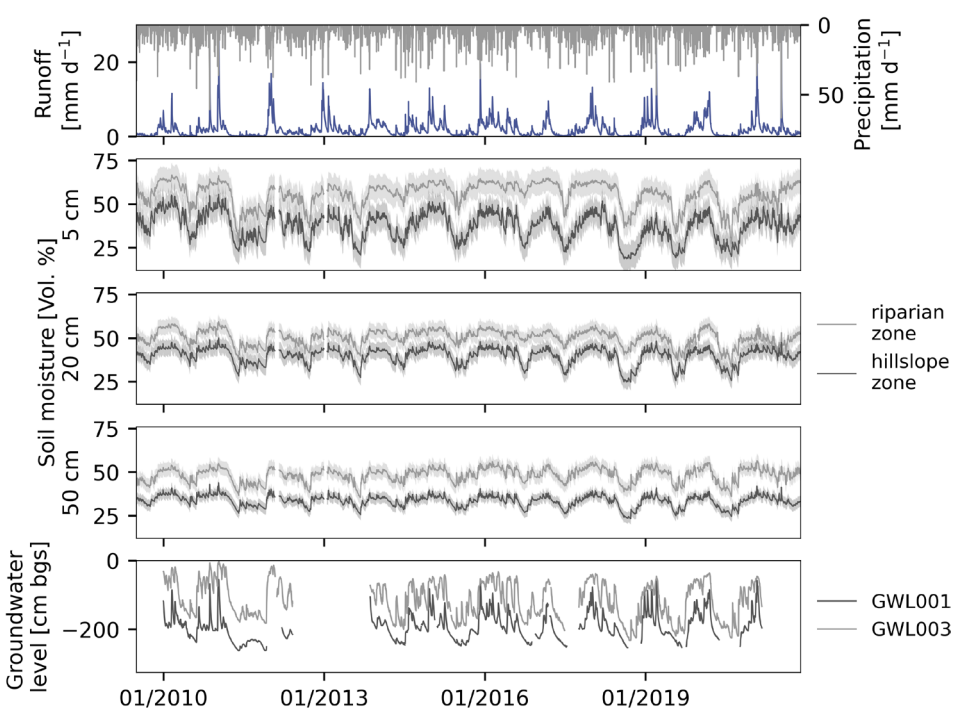


FIGURE 2 | Time series of observed daily precipitation (grey bars from top), runoff at the catchment's outlet (blue), volumetric soil moisture in 5, 20 and 50 cm for the hillslope zone (dark grey) and the riparian zone (light grey) and groundwater level for station GWL 001 (dark grey) and GWL003 (light grey) in the forest catchment. Grey bands for soil moisture data indicate the spatially averaged soil moisture value ± the standard deviation.

2.2.1 | Precipitation and Runoff

Daily runoff and precipitation were measured from July 2009 to December 2021 in the forest, from January 2010 to October 2022 in the grassland and from May 2010 to December 2019 in the agricultural catchment. In the forest and grassland catchments, runoff was recorded with a V-notch weir for low flows and a Parshall flume for medium to high flows (Bogena et al. 2015; Qu et al. 2016), while in the agricultural catchment, an H-flume was used (Blöschl et al. 2016). Daily precipitation data for the forest catchment was provided by the Monschau-Kalterherberg meteorological station (DWD, station number 3339). For the grassland catchment, precipitation was acquired from a rain gauge (weighing OTT Pluvio) installed in July 2013 in the centre of the catchment and from a Hellmann-type tipping bucket at the outlet from January 2010 to July 2013. Due to low spatial variability between the four available rain gauges (weighing OTT Pluvio) in the agricultural catchment (Vreugdenhil et al. 2022), we calculated daily precipitation as the arithmetic mean of the four gauges.

2.2.2 | Soil Moisture

Daily soil moisture was available in the forest catchment from July 2009 to December 2021, in the grassland catchment from March 2011 to October 2022 and in the agricultural catchment from July 2013 to December 2019. We used soil moisture data from the SoilNet wireless sensor network installed in the forest catchment in 2009, recorded every 15 min at 5, 20 and 50 cm depth at 150 sites with EC-5 soil moisture sensors (METER Group GmbH, Munich, Germany; Rosenbaum et al. 2012), of which we selected 108 for further analysis based on previous quality controls (Bogena et al. 2010; Wiekenkamp et al. 2016a). In the grassland catchment,

soil moisture was measured from 2011 until May 2015 at 87 sites at the same depths using a SoilNet equipped with SPADE soil moisture sensors (Qu et al. 2013, 2016). Due to technical problems, the SPADE sensors were replaced by SMT100 soil moisture sensors at 41 SoilNet sites from 2014 onwards (Bogena et al. 2017), of which we selected 33 stations with continuous data (TERENO 2024). In the agricultural catchment, 32 SoilNet stations equipped with SPADE soil moisture sensors were operated from mid-2013 to late 2021, of which we selected 29 sensors after checking for continuity and outliers. In the forest catchment, we averaged soil moisture in the three depths separately for the riparian and hillslope zones, as the two zones can be accurately delineated based on the predominant soil types, and sensors were available in both zones. Due to the low density of sensors near the stream in both the grassland and agricultural catchments, we calculated spatial averages of soil moisture in the three depths over the entire catchment area. Additionally, we calculated a depth-weighted mean for a soil depth of 1m assuming a depth-dependent soil moisture variability in all catchments (following Stockinger et al. 2014), with the largest weight of 0.7 given to the measurement at 50cm, and weights of 0.2 and 0.1 to the measurements at 20 and 5 cm, respectively. Since additional soil moisture measurements at 10cm in the agricultural catchment were available, we included them in the depth-weighted mean accordingly, with 5 and 10 cm each receiving a weight of 0.05.

2.2.3 | Groundwater Level

In the forest catchment, we selected two groundwater level measurement sites (Bogena et al. 2015) that showed the best continuity from January 2010 to March 2021. Both stations are located in the riparian zone of the catchment, with station GWL003 upstream near the stream in the deforested zone and GWL001 further

downstream in the forested area (Figure 1). In the agricultural catchment, station H09 recorded groundwater levels from May 2011 to December 2019 and lies in the riparian zone on a lower slope, representing the transition between riparian and hillslope zones (Pavlin et al. 2021; Vreugdenhil et al. 2022). We also selected piezometer BP01, which is situated close to the stream, with data from December 2012 to December 2019 and minimal gaps. Other stations in the agricultural catchment behaved similarly to either H09 or BP01, so that we anticipated the two piezometers to be representative of the catchment. As the groundwater in the grassland catchment is confined and restricted to deep, fractured rocks, no groundwater level observations were available.

3 | Methods

3.1 | Time Series-Based Soil Moisture Pattern Search

We analysed the influence of hydro-meteorological variables on event runoff characteristics on the daily time scale by implementing a time series-based pattern search in each catchment individually (Figure 3).

3.1.1 | Runoff Event Identification

We identified rainfall-runoff events (Figure 3a) by employing the Detrending Moving-average Cross-correlation Analysis-Event Separation Routine (DMCA-ESR; Giani et al. 2022). Essentially, the method makes use of the centre of mass of rainfall and runoff time series fluctuations to simultaneously identify rainfall-runoff events. In detail, it first determines the typical catchment response time (Giani et al. 2021), which is used as a constraining window to calculate the time series of rainfall and runoff fluctuations. Rainfall-runoff events are then identified as periods where both rainfall and streamflow exceed a pre-defined fluctuation tolerance threshold (Giani et al. 2022). The method does not require subjective parameter choices and has been successfully applied in other catchmentscale studies (e.g., Zheng et al. 2023). Further, it does not require a priori base flow separation; the base flow component is separated after identification for each event by taking the minimum runoff before the rising limb (Giani et al. 2022). We excluded events falling below the mean runoff, which has been adopted by previous studies as a meaningful threshold for runoff event identification (e.g., Hövel et al. 2024a; Zheng et al. 2023).

3.1.2 | Similarity of Soil Moisture and Runoff Patterns

For each runoff event, we extracted the concurrent depthweighted mean soil moisture (Figure 3b) and used it to find analogous soil moisture patterns at different times in the same catchment (Figure 3c). A soil moisture pattern was therefore defined as a segment of the soil moisture time series with a certain duration. The term *analogous* was used for soil moisture patterns to avoid confusion with *similar* runoff patterns later on. We applied the Matrix Profile method, which

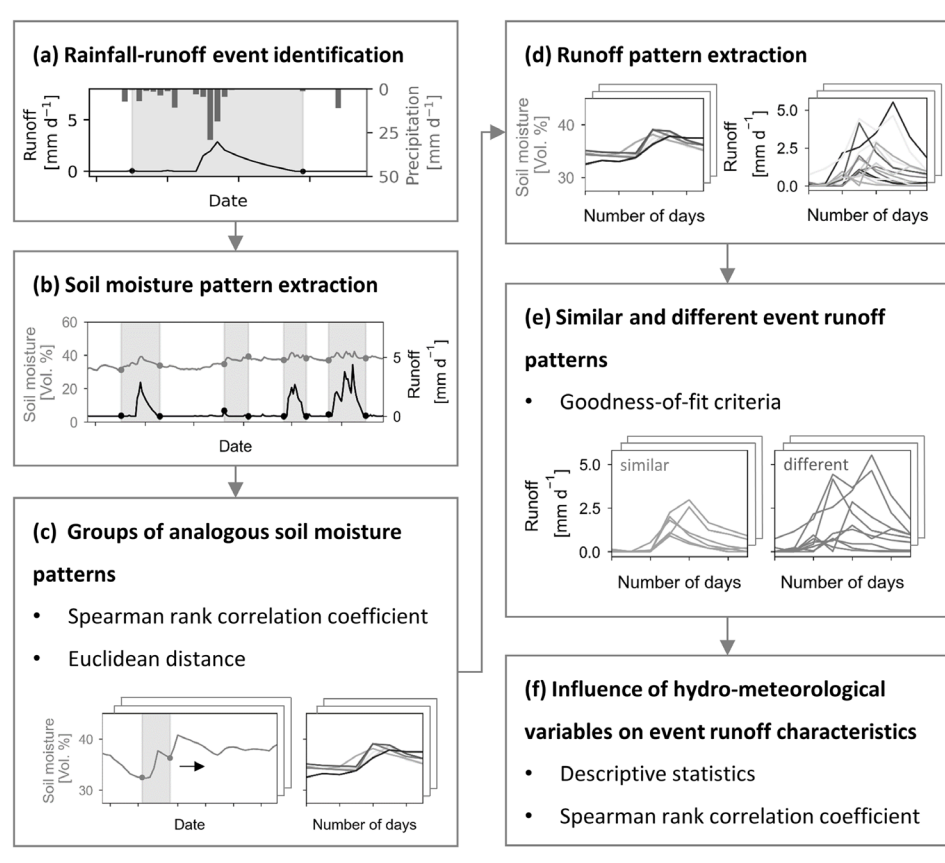


FIGURE 3 | Flow chart of the time series-based pattern search in soil moisture and overview of the runoff characteristics and hydro-meteorological variables used in the analysis.

Runoff characteristics • Event runoff coeffi

- Event runoff coefficient ERC
- Event timescale Ts
- Recession coefficient Rc
- Normalized peak runoff Qmax

Hydro-meteorological variables

- Rainfall-derived variables
 Psum, Pmax, Pint
- Potential evapotranspiration
 PET
- Antecedent soil moisture
 ASM5, ASM20, ASM50
 in three depths of 5 cm,
 20 cm, and 50 cm,
 respectively
- Antecedent groundwater level GWLpre

TABLE 1 | Event runoff characteristics used as target variables.

Variable	Abbreviation	Definition	Equation	References
Event runoff coefficient	ERC [-]	Ratio of the event runoff volume [mm] to the event rainfall volume [mm]	$ERC = \frac{Q_{\text{vol}}}{P_{\text{vol}}}$	Merz et al. (2006), Sherman (1932)
Event timescale	$T_{\rm s}$ [days]	Ratio of event runoff volume [mm] to the daily peak runoff [mm d ⁻¹]	$T_{\mathrm{S}} = rac{Q_{\mathrm{vol}}}{Q_{\mathrm{peak}}}$	Gaál et al. (2012)
Recession coefficient	R _c [-]	Exponent b in the power law recession model	$\frac{\mathrm{d}Q}{\mathrm{d}t} = -aQ^b$	Brutsaert and Nieber (1977), Dralle et al. (2015, 2017)
Normalised peak runoff	$Q_{\max}[-]$	Maximum daily peak runoff [mm d^{-1}] normalised by the long-term mean runoff [mm d^{-1}]	$Q_{\text{max}} = \frac{Q_{\text{peak}}}{\overline{Q}}$	Tarasova, Basso, Zink, et al. (2018)

was developed to robustly identify all patterns that match a specific pattern in the time series (Madrid et al. 2019; Yeh et al. 2016). We defined two criteria to assess the similarity of soil moisture patterns: (1) they exceeded a Spearman rank correlation coefficient threshold of 0.76, 0.74 and 0.53 in the forest, grassland and agricultural catchments, respectively (adapted from Hövel et al. 2024a), and (2) the Euclidean distance between them was lower than 5 vol% to account for absolute deviations between patterns. The correlation coefficient thresholds represent the mean correlation between soil moisture patterns of similar runoff events (Hövel et al. 2024a) and were therefore used as a threshold. To assess how the results obtained changed with variations in the two similarity criteria, we conducted a (one-at-a-time) sensitivity analysis given in Supporting Information S2. Consequently, groups of analogous soil moisture patterns were derived. Since the groups were based on the depth-weighted mean soil moisture, we additionally assessed the relationship between soil moisture patterns in the three measurement depths of 5, 20 and 50 cm by calculating the Pearson correlation coefficient (r) and evaluating its significance on a 95% confidence level (p < 0.05).

For each group of analogous soil moisture patterns, we extracted the respective runoff patterns from the time series. An event runoff pattern was therefore defined as a segment of the runoff time series with a certain duration and at least one runoff peak on a given day. Based on goodness-of-fit criteria, one group of similar and one group of different runoff patterns were derived for each group of analogous soil moisture (Figure 3e). We combined the Nash–Sutcliffe Efficiency (NSE; Equation (1)), with a volume error (VE; Equation (2)) to form the NVE as suggested by Lindström (1997):

NSE = 1 -
$$\frac{\sum_{i=1}^{n} (Q_1 - Q_2)^2}{\sum_{i=1}^{n} (\overline{Q}_2 - Q_2)^2}$$
 (1)

$$VE = \frac{\sum_{i=1}^{n} |Q_1 - Q_2|}{\sum_{i=1}^{n} Q_2}$$
 (2)

$$NVE = NSE - \chi |VE|$$
 (3)

 Q_1 and Q_2 represent the respective event runoff patterns, with \overline{Q} denoting the mean over the pattern duration (n days). The parameter χ serves as a weighting factor for the VE set to 0.1, according to Lindström (1997). We defined patterns to be similar if the NVE exceeded a threshold of 0.65. As this threshold is widely considered a 'satisfactory' or 'good' fit between runoff time series for the NSE (Moriasi et al. 2007; Saleh et al. 2000; Singh et al. 2005), we assumed it to be applicable to the NVE as well. At the same time, event runoff patterns were classified as different if they did not fulfil the similarity criterion. For example, they were not similar to any other runoff pattern extracted for the respective soil moisture group (Figure 3e). An example of the derived groups of runoff patterns can be found in Supporting Information S3. In the subsequent analysis, we focused only on groups of soil moisture patterns for which both similar and different runoff patterns could be identified.

3.2 | Runoff Characteristics

For all runoff patterns, we assessed four descriptive characteristics (Table 1): the ERC, the daily peak runoff normalised by the long-term mean runoff (Q_{max}), the ratio of runoff volume to the daily peak runoff (T_s) and the recession coefficient (R_c) . Further details on the estimation of the recession coefficient $R_{\rm s}$ are given in Supporting Information S4. We calculated the four runoff characteristics for each runoff pattern individually and then averaged them over each group of analogous soil moisture patterns (Figure 3d). We allocated the meteorological seasons of spring (March, April and May), summer (June, July and August), autumn (September, October and November) and winter (December, January and February) to all patterns based on their first day of occurrence. To test for differences in runoff characteristics between seasons, we conducted a Kruskal-Wallis test followed by Dunn's post hoc test. Furthermore, we calculated the mean runoff characteristics of similar and different runoff patterns separately and indicated the coefficient of variation (CV) for all respective mean characteristics. To test for differences between the two groups, we applied a Wilcoxon rank-sum test. The statistical test results were evaluated using a 95% confidence level (p < 0.05).

3.3 | Hydro-Meteorological Variables

Rainfall-derived variables included the event rainfall sum $P_{\rm sum}$ [mm], the maximum event rainfall intensity $P_{\rm max}$ [mm d⁻¹] and the event mean rainfall intensity $P_{\rm int}$ [mm d⁻¹]. Furthermore, we calculated the event mean PET [mm d⁻¹] with the Penman–Monteith equation. In terms of wetness-derived variables, we assessed the impact of ASM 1 day before the event ASM5, ASM20 and ASM50 [vol. %] in measurement depths of 5, 20 and 50 cm, respectively. Additionally, we calculated the groundwater level 1 day before the event GWLpre [cm bgs] in the forest and agricultural catchments. To analyse how hydro-meteorological variables influenced the runoff patterns in respective seasons, we used the Spearman rank correlation coefficient (ρ) and evaluated its significance based on a 95% confidence level (p<0.05).

4 | Results

4.1 | Time Series-Based Soil Moisture Pattern Search

A total of 100, 95 and 120 runoff events and concurrent soil moisture patterns (Figure 3b) were extracted in the forest, grassland and agricultural catchments, respectively. Only considering soil moisture patterns for which similar and different runoff patterns were identified (Figure 3e), 62, 16 and 55 groups of analogous soil moisture patterns were formed in the three catchments, respectively. Particularly in the forest catchment, we observed a high average number of matches for one soil moisture pattern (Supporting Information S5). Thus, soil moisture patterns were not restricted to times when runoff events were identified but were distributed across the entire time series. While in the forest and grassland catchments, most groups consisted of wetting and subsequent drying patterns, soil moisture patterns in the agricultural catchment mainly comprised wetting-up patterns with higher variability within a group than in the other catchments, as shown by the broad confidence intervals (Supporting Information S6). In the grassland catchment, we particularly observed consistent wetting-up and drying patterns of soil moisture with one distinct peak for most groups (Figure 4). Although in the forest catchment, most groups showed a similar pattern to the grassland catchment; there were also patterns with slower drying after the peak compared to the rest of the groups (Supporting Information S6).

Regarding the different soil moisture measurement depths for the identified patterns, we found a strong significant correlation between the soil moisture in 5 and 20 cm depth in the forest (r=0.83) and agricultural (r=0.72) catchments, but not in the grassland catchment (r=0.31). While correlation coefficients remained low between soil moisture in 5 and 50 cm in the grassland and agricultural catchments (Supporting Information S7), soil moisture in the two layers was significantly correlated in the forest catchment at 0.61. The percentages of the runoff patterns attributed to either the group of similar or different runoff for each group of analogous soil moisture patterns differed between the catchments. In the agricultural catchment, the average number of similar

runoff patterns for one soil moisture pattern was higher than the number of different patterns, in contrast to the other two catchments (Supporting Information S5).

4.2 | Runoff Characteristics and Their Seasonality

The forest and grassland catchment had overall comparable runoff characteristics under analogous soil moisture patterns, particularly in terms of mean ERC (0.25 and 0.27, respectively) and timescales $T_{\rm s}$ (5.08 and 4.42 days, respectively) (Table 2). In contrast, the agricultural catchment showed lower mean ERC and shorter $T_{\rm s}$ compared to the other two catchments, with 0.09 and 2.38 days, respectively, with ERC having the largest CV of all runoff characteristics in the catchment at 0.73. In the forest catchment, we observed the highest CV for the recession coefficient $R_{\rm c}$ with 1.20, while in the grassland catchment, CV was largest for the normalised peak runoff $Q_{\rm max}$ at 0.80 (Table 2).

The runoff characteristics in the three catchments varied throughout the year: ERC in the forest and agricultural catchment followed a seasonal pattern, as for the differentiation between similar and different runoff patterns, with ERC being highest in winter and lowest in summer (Figure 5). In both catchments, ERC differed significantly between almost all seasons, except between spring and summer in the forest catchment. In contrast, ERC in the grassland catchment did not vary considerably between the two seasons of summer and autumn as well as spring and winter (Supporting Information S8).

 $T_{\rm s}$ in the forest and grassland catchments followed the same seasonality as ERC, with longer $T_{\rm s}$ in spring and winter compared to the rest of the year (Supporting Information S8 and S9). In contrast, $T_{\rm s}$ in the agricultural catchment showed no major seasonal variations (CV = 0.32) and was, on average, shorter (~2 days) than in the forest (~5 days) and grassland (~4.5 days) catchments. On average, we found the largest Rc in the agricultural catchment in winter, whereas in the forest and grassland catchments, $R_{\rm c}$ was highest in the summer (Supporting Information S9).

4.3 | Linking Hydro-Meteorological Variables and Their Seasonal Dynamics With Runoff Characteristics

4.3.1 | Similar Runoff Patterns

For similar runoff patterns, all runoff characteristics were, on average, significantly correlated with wetness-derived variables in the forest (ASM50) and grassland catchments (ASM5), while in the agricultural catchment, only ERC and $R_{\rm c}$ were primarily correlated with these. Figure 6 displays the Spearman rank correlation coefficients (ρ) between runoff characteristics and hydro-meteorological variables in the three catchments, differentiated between similar and different runoff.

ERC was significantly correlated with ASM in 50cm in both the riparian (ρ =0.58) and hillslope (ρ =0.58) zones in the forest catchment and in the agricultural catchment (ρ =0.56). In

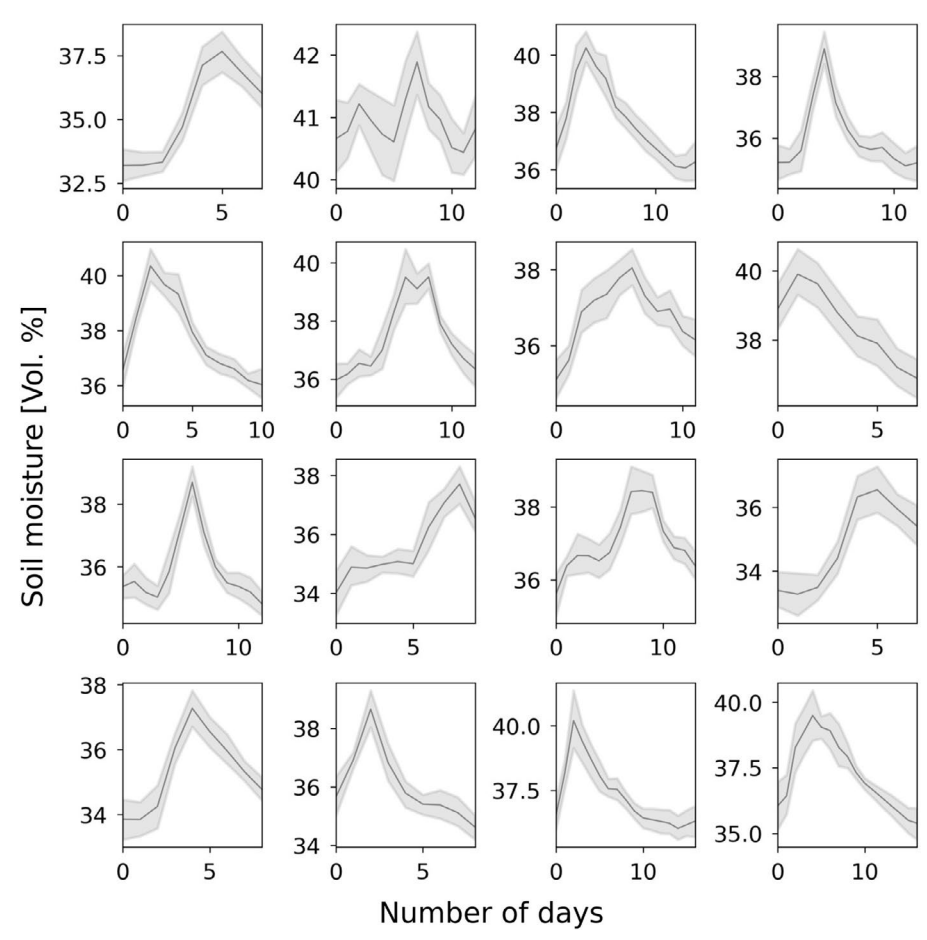


FIGURE 4 | Groups of analogous soil moisture patterns in the grassland catchment, indicating the mean soil moisture in each group and the corresponding 95% confidence interval.

TABLE 2 | Descriptive statistics of runoff characteristics averaged over all runoff patterns in the respective groups of analogous soil moisture patterns detected in the three catchments, including their mean and coefficient of variation (CV).

		Forest catchment	Grassland catchment	Agricultural catchment
ERC [-]	Mean	0.25	0.27	0.09
	CV	0.88	0.72	0.73
$T_{\rm s}$ [days]	Mean	5.08	4.42	2.38
	CV	0.49	0.46	0.32
$R_{\rm c}$ [-]	Mean	0.75	0.98	1.02
	CV	1.20	0.76	0.41
$Q_{\max}[-]$	Mean	4.71	6.37	18.61
	CV	1.08	0.80	0.56

comparison, in the grassland catchment, it was correlated with ASM in 5 cm (ρ = 0.52). In all catchments, we observed a threshold relationship of ERC with ASM in the respective depths, with ERC and ASM being seasonally related for similar runoff patterns: Soil moisture in summer rarely reached a threshold after which ERC substantially increased, so that ERC generally remained low. In contrast, the largest ranges of ERC with values from 0 to 1 occurred in winter (Figure 7). The thresholds in ASM, determined with a segmented linear regression, were approx. 46.8 and 32.0 vol% in 50 cm soil depth in the riparian

and hillslope zones of the forest catchment, respectively, and 48.2 vol% in 5cm and 37.4 vol% in 50cm in the grassland and agricultural catchment, respectively (Figure 7).

In addition to ASM, we found a significant correlation between ERC and pre-event groundwater levels (GWLpre) at both piezometers in the forest catchment (ρ =0.49 and ρ =0.53 at GWL001 and GWL003, respectively). Similarly, ERC and GWLpre at H09 and BP01 were significantly correlated in the agricultural catchment (ρ =0.33 and ρ =0.34, respectively) with

seasonal differences of higher groundwater levels and ERC in the winter season compared to the other seasons. Furthermore, the nonlinearity of recession, $R_{\rm c}$, had the highest correlations with wetness-derived variables compared to the other hydrometeorological variables in the forest and agricultural catchments for similar runoff patterns. In the forest catchment, ASM50 in the hillslope zone was significantly correlated with

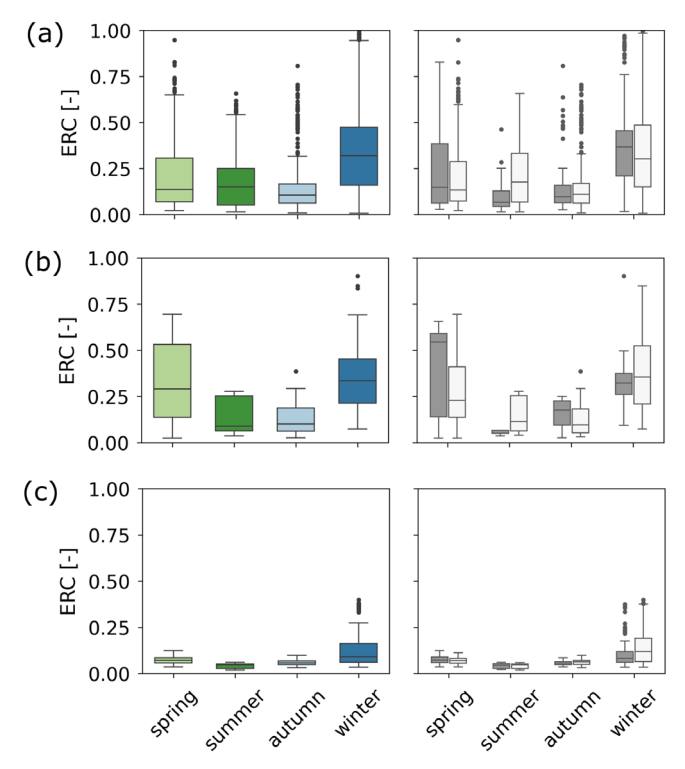


FIGURE 5 | Event runoff coefficient (ERC) for spring, summer, autumn and winter, including all runoff patterns in the left column and separated between similar (grey) and different (light grey) runoff patterns in the right column for the (a) forest, (b) grassland and (c) agricultural catchments, respectively.

 $Rc~(\rho\!=\!-0.47).$ In addition, Rc was correlated with the pre-event GWL at piezometer H09 in the agricultural catchment. In the forest catchment, groundwater levels and ASM in deep layers were additionally correlated with $Q_{\rm max}$ and $T_{\rm s}.$ In the grassland catchment, ASM in 5 cm showed the highest significant correlation with $Q_{\rm max}~(\rho\!=\!0.53).$ In both the forest and grassland catchments, we found $T_{\rm s}$ of similar runoff patterns to be positively correlated with rainfall sums $P_{\rm sum}.$ Furthermore, rainfall characteristics were the only variables correlated with $Q_{\rm max}$ in the agricultural catchment and showed a positive correlation with $Q_{\rm max}$ in the forest catchment.

4.3.2 | Different Runoff Patterns

In the forest and grassland catchments, correlation coefficients were in most cases lower in the group of different runoff patterns compared to the similar ones. If not, differences were marginal (e.g., $\rho = 0.15$ and $\rho = 0.20$ between ERC and P_{max} in the forest catchment for similar and different runoff patterns, respectively). Meanwhile, we found a significant positive correlation between $Q_{\rm max}$ and rainfall volumes $P_{\rm sum}$ and intensities $P_{\rm int}$ for different runoff patterns, with values of 0.58 and 0.56 for P_{sum} and 0.58 and 0.53 for P_{int} in the forest and grassland catchments, respectively (Figure 6). Furthermore, the threshold relationship between ERC and ASM observed in both catchments was not as pronounced for different runoff patterns (Supporting Information S10) as for similar patterns. For instance, we observed an increased ERC of 0.6 for low ASM in the hillslope zone (ASM50 around 33 vol%) in the forest catchment. On the contrary, the agricultural catchment also showed a pronounced threshold relationship between ERC and ASM50 for different runoff patterns (Supporting Information S10). In general, we found higher correlation coefficients for different rather than similar runoff patterns more frequently in the agricultural catchment than in the other two catchments. This was particularly evident for the runoff characteristics of ERC, $R_{\rm c}$ and $Q_{\rm max}$: correlation coefficients were larger between ERC and groundwater

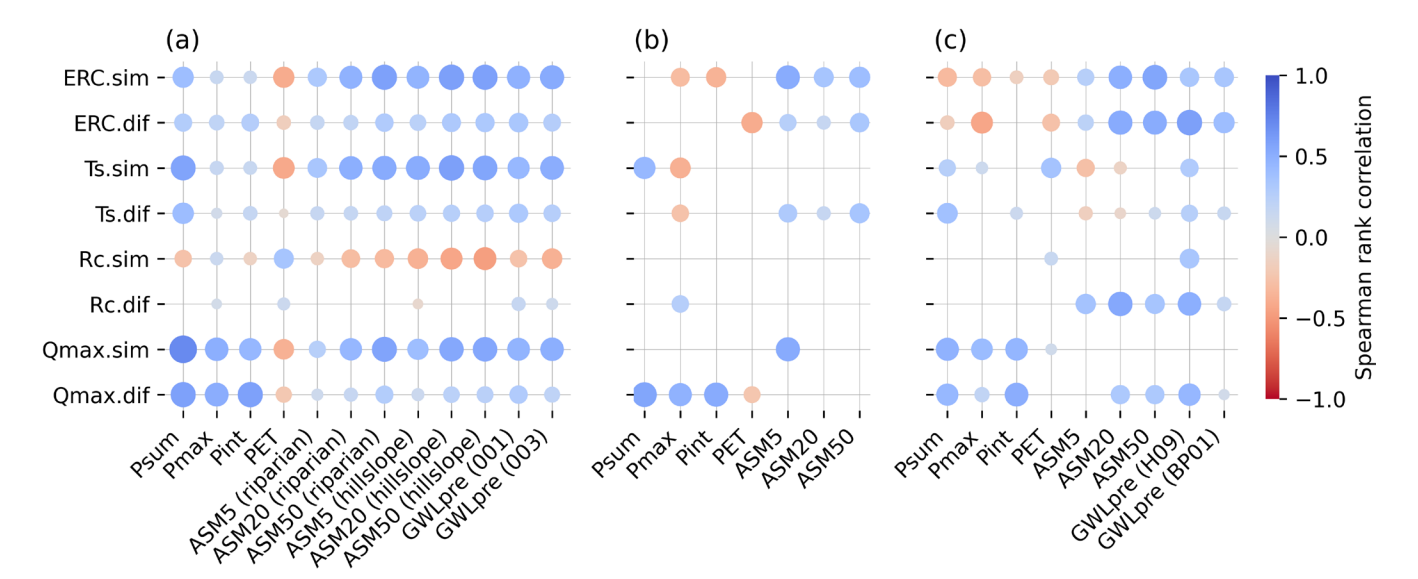


FIGURE 6 | Heatmap showing Spearman rank correlation coefficients (ρ) between event runoff characteristics and selected hydro-meteorological variables (p < 0.05), separated between groups of similar (e.g., ERC.sim) and different (e.g., ERC.dif) runoff patterns in the (a) forest, (b) grassland and (c) agricultural catchments, respectively. The size and colour of the dots both indicate the value of the correlation coefficient for better visualisation.

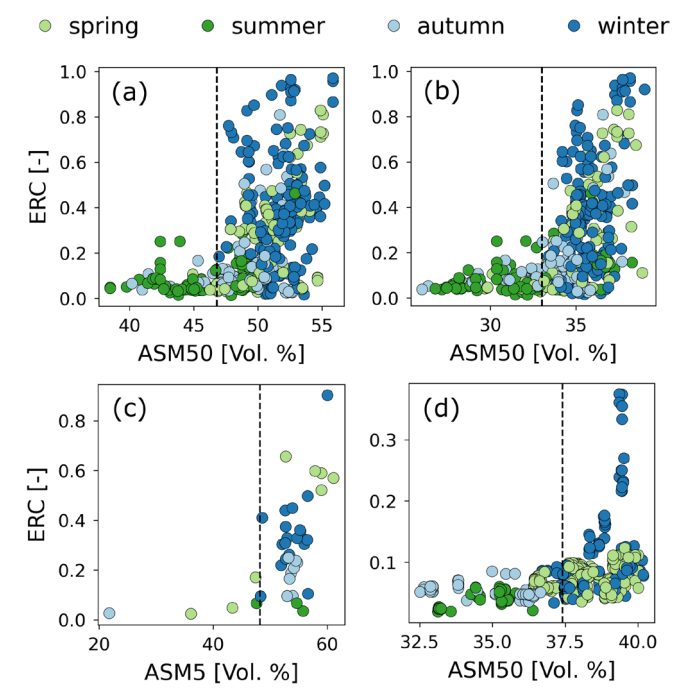


FIGURE 7 | Relationship between antecedent soil moisture (ASM) and event runoff coefficient (ERC) in (a) the riparian zone and (b) the hillslope zone of the forest catchment in $50\,\mathrm{cm}$ (ASM50), (c) in the grassland catchment in $5\,\mathrm{cm}$ (ASM5) and (d) in the agricultural catchment in $50\,\mathrm{cm}$ (ASM50), for similar runoff patterns. The vertical dashed lines in each panel indicate the threshold in ASM determined with a two-step segmented linear regression.

levels in the agricultural catchment for different runoff patterns compared to similar ones. Likewise, we observed higher correlations between $R_{\rm c}$ and wetness-derived variables for different runoff patterns than similar ones, with ASM20 having the highest correlation with $R_{\rm c}$ ($\rho\!=\!0.54$). In addition to rainfall-derived variables, wetness-derived variables showed increased correlations with $Q_{\rm max}$ for different runoff patterns compared to similar ones in the agricultural catchment (Figure 6). In contrast, in the other two catchments, particularly in the grassland, wetness-derived variables did not show any significant correlation with $Q_{\rm max}$ for different runoff patterns.

5 | Discussion

5.1 | Temporal Patterns in Soil Moisture and Their Linkage to Respective Runoff Patterns

Different analogous soil moisture patterns were found during runoff events and during dry conditions because not only rainfall-driven wetting but also radiation-driven drying influences soil moisture dynamics (Liu et al. 2024; Mälicke et al. 2020). The largest number of analogous soil moisture patterns was in the forest catchment, indicating low variability and therefore high recurrence of the wetting and subsequent drying cycles. Although soil moisture patterns in the grassland catchment showed similar wetting-up and drying cycles (Figure 4), comparatively few repeating ones were found. As soil moisture patterns in 5 cm were not well correlated with those in 20 cm (r=0.31) or 50 cm depth (r=0.39), the large weights of both 20

and 50 cm soil moisture in the depth-weighted mean might have resulted in fewer recurrent soil moisture patterns in the grassland catchment. In contrast to the other two catchments, patterns of analogous soil moisture in the agricultural catchment were more variable, as indicated by the broad confidence intervals within the groups (Supporting Information S6). The large variability of soil moisture patterns within one group may also result from the comparably low correlation coefficient we set as a similarity criterion for the soil moisture patterns to match (ρ =0.53). Most patterns did not follow a clear wetting and drying, but rather a continuous wetting-up, with the soil moisture peak following the runoff peak (Supporting Information S6), as also reported by Pavlin et al. (2021) for the agricultural catchment.

As for the respective runoff patterns, the majority of runoff under analogous soil moisture patterns in the forest and grassland catchments was classified as different (Supporting Information S5), showing that runoff patterns were variable over time. In contrast, in the agricultural catchment, although analogous soil moisture patterns showed high variability, the group of similar runoff was on average larger than the one of different patterns. This suggests an increased number of similar runoff patterns in the catchment compared to the forest and grassland catchments, as also indicated by the high number of clusters containing similar runoff events (Hövel et al. 2024a). Even though runoff mechanisms in different sub-parts of the agricultural catchment are complex (Vreugdenhil et al. 2022), our study demonstrated that the catchment average runoff response at the outlet shows a high degree of repeatability over time.

5.2 | Hydro-Meteorological Drivers of Event Runoff Characteristics and Their Linkage to Catchment Wetness States

5.2.1 | Influence of Rainfall-Derived Variables on Runoff Characteristics

Rainfall characteristics, particularly $P_{\rm sum}$ and $P_{\rm int}$, likely impacted runoff characteristics of ERC, $T_{\rm s}$ and $Q_{\rm max}$ in the catchments studied. In the forest and grassland catchments, rainfall sums $P_{\rm sum}$ showed a positive correlation with $T_{\rm s}$ of similar runoff patterns, suggesting a potential influence on the runoff response shape, with a higher P_{sum} leading to a longer T_{s} . In addition, Q_{max} for different runoff patterns showed a significant positive correlation with $P_{\rm sum}$ and $P_{\rm int}.$ A strong positive correlation between rainfall volumes and Q_{max} was also found by Tarasova, Basso, Zink, et al. (2018), possibly hinting at a wet catchment state leading to an increase in ERC (Berghuijs et al. 2016). Conversely, we observed a significant negative correlation between rainfall and ERC in the agricultural catchment, where even low $P_{\rm sum}$ led to high ERC, which was possibly triggered by long, consistent, low-intensity rainfall events in winter times (Supporting Information S10). This somewhat counterintuitive observation is supported by the findings of Merz and Blöschl (2009) in other Austrian catchments, for which low maximum rainfall intensities also led to high ERC. They attributed this phenomenon to the rainfall characteristics in Austria, with rainfall events of longer duration leading to higher runoff coefficients than shorter,

more intensive rainfall events. Furthermore, $P_{\rm sum}$ and $P_{\rm int}$ were equally correlated with $Q_{\rm max}$ of similar and different runoff patterns in the agricultural catchment, indicating a potential control of the two rainfall characteristics on the normalised peak runoff regardless of the observed hydrograph shape. Still, similar shapes of the runoff response at the catchment's outlet were also influenced by the temporal precipitation pattern (Hövel et al. 2024a). The potentially dominant control of rainfall characteristics on the runoff response in the agricultural catchment is further supported by Szeles et al. (2024), who found a high contribution of new water (~50%) during peak flows, suggesting a rapid contribution of precipitation to the stream via surface runoff. Surface runoff in the catchment may occur for various reasons, with agricultural land use and soil compaction being one of the major influencing factors (Szeles et al. 2024).

5.2.2 | Influence of Wetness-Derived Variables on Runoff Characteristics

In the forest catchment, ASM50 and GWLpre likely influenced runoff characteristics of similar runoff patterns. GWLpre at both stations showed similar correlations with runoff characteristics, although only GWL003 was influenced by deforestation. Previous studies indicated that the catchment response to vegetation alterations is highly variable over time (e.g., Hornbeck et al. 1993; Andréassian 2004). In the catchment studied, deforestation caused a decrease in evapotranspiration and an increase in soil water storage in the deforested area (Wiekenkamp et al. 2016a), possibly leading to a higher percolation. Furthermore, the strong correlation of ASM in deep soil layers may be explained by macropores allowing deeper infiltration in forest soils compared to grasslands (e.g., Alaoui et al. 2011). Thus, precipitation reaching deeper soil layers might have contributed to the catchment's runoff as subsurface stormflow. Wiekenkamp et al. (2016b) observed catchmentwide preferential flow during both relatively dry and extremely wet conditions in the forest catchment. Similar results have been reported by Vichta et al. (2024) in a forested headwater catchment, highlighting the role of trees in transporting water to deeper soil layers via preferential flow paths. Our results in the forest catchment, therefore, suggest an overall fast pressure response between soil moisture, groundwater level, and the stream due to potentially high hydraulic conductivity and preferential flow paths in the subsurface, resulting in similar runoff patterns at the catchment's outlet. Isotope data analysed in the catchment further support this observation, where streamflow was found to substantially consist of groundwater, and the fraction of water younger than 3 months was generally low at approx. 10% (Stockinger et al. 2019). Furthermore, runoff generation often depends on a threshold in ASM (e.g., Detty and McGuire 2010; VanTromp-Meerveld and McDonnell 2006); this was also found in the forest catchment, where the hillslope zone contributes to runoff only above a soil moisture threshold (Stockinger et al. 2014). An increase in ERC was only apparent after a certain soil moisture threshold was reached, predominantly in spring and winter (Figure 7), and below this threshold, no runoff event was triggered, indicating significant subsurface storage capacity. This storage capacity is confirmed by model results of Hrachowitz et al. (2021) in the forest catchment; they suggest a storage volume of at least ~8000 mm in the

layered and fractured Devonian shale bedrock. However, the high storage capacity may also be due to the subsurface being connected to surrounding areas outside the boundaries of the surface catchment area. In addition to the potentially large storage capacity, the threshold relationship between ERC and ASM may also be reinforced by water losses due to evapotranspiration during periods when hydrological connectivity was not established. This is further corroborated by the results of our correlation analysis, which showed that an increase in PET led to a decrease in ERC.

The potential dominant role of ASM in the grassland catchment in the topsoil rather than the deep layer may be due to increased bulk density and reduced percolation of water (Alaoui et al. 2011; Li and Shao 2006). In this regard, Alaoui et al. (2011) suggested that the limited vertical water transport in grasslands may partly be due to the finer and denser soil structure in the topsoil as a result of the prevalent land use. In the grassland catchment, Qu et al. (2016) showed that bulk density increased with soil depth based on 273 soil samples. The strong correlations between ASM5 and ERC, $T_{\rm s}$ and $Q_{\rm max}$ might therefore be due to fast interflow close to the surface resulting from higher hydraulic conductivity in the upper soil layer compared to the deeper layers.

In the agricultural catchment, the threshold relationship between ERC and ASM50 held for both similar and different runoff patterns, indicating that this relationship likely controlled ERC of all runoff patterns. Still, ERC and $Q_{\rm max}$ for different runoff patterns may additionally be influenced by water bypassing the soil or preferential flow through the installed tile drains in the catchment. In terms of seasonality, small rainfall sums combined with high ASM leading to high ERC also hint at consistent subsurface connectivity during wet winter months, as also indicated by Széles et al. (2018) and Vreugdenhil et al. (2022). However, the catchment's overall shorter Ts and therefore flashier response (2.4days) compared to the other two catchments indicate a decreased soil storage capacity due to shallow soils with medium to poor infiltration capacities (Blöschl et al. 2016; Gaál et al. 2012; Vreugdenhil et al. 2022). In addition, the earlier response of the stream compared to the soil moisture might indicate overland flow processes. Similar observations were reported by Beiter et al. (2020) in an agricultural catchment located in central Europe. The significant correlations between $Q_{\rm max}$ and $P_{\rm int}$ for both similar and different runoff patterns further support the presence of infiltration-excess overland flow. Furthermore, we found significant correlations between runoff characteristics, particularly ERC, and GWLpre at H09 and BP01 $(\rho = 0.59 \text{ and } \rho = 0.40, \text{ respectively})$ for different runoff patterns, suggesting that groundwater contributes to the stream most times of the year (Eder et al. 2022; Exner-Kittridge et al. 2016). Our results, therefore, indicate that both overland flow and subsurface flow may potentially occur at different times in the catchment. Similarly, Vreugdenhil et al. (2022) suggested that in winter and spring, shallow flow paths such as overland flow may dominate in the catchment, while in summer, contributions from deeper flow paths to the stream may be more likely.

 $R_{\rm c}$ and ASM20 in the agricultural catchment were significantly correlated for different runoff patterns (ρ =0.54). The non-linearity in recession increased from dry to wet catchment states, that is, when riparian-hillslope connectivity was reached,

which was also found in mountainous catchments (Harman et al. 2009; Lee et al. 2023). However, in the forest and grassland catchments, we observed the opposite relationship with a significant negative correlation between R_c and ASM50 for similar runoff patterns. Saffarpour et al. (2016) also suggested that recession is slower the wetter the catchment, and vice versa, leading to the observed shorter timescale during dry conditions, which was additionally found by Latron and Gallart (2008). Furthermore, Gaál et al. (2012) suggested that a short timescale in dry conditions may be due to more efficient drainage compared to wet catchment conditions, even for high rainfall sums. The increased recession non-linearity and shorter timescales in the forest catchment in dry conditions may additionally be amplified by evapotranspiration effects ($\rho = 0.35$). Yet, we found that PET generally played only a minor role in influencing runoff characteristics in the three catchments studied, potentially due to the short-term temporal scales analysed. Thus, the use of long-term predictors such as the aridity index in addition to the short-term, pattern-based PET in our analysis could potentially provide further insights into the role of PET.

5.3 | Limitations and Possible Future Applications

In the past, most studies analysing catchment-scale temporal patterns either focused on soil moisture without considering respective event runoff characteristics (Korres et al. 2015; Liu et al. 2024; Mälicke et al. 2020; Rosenbaum et al. 2012) or only investigated runoff patterns (e.g., Gaál et al. 2016). Here, we directly linked runoff and soil moisture through the pattern search, with the soil moisture patterns based on the times when runoff events were identified. Similarly, Araki et al. (2022) linked soil moisture to runoff and suggested that particularly event-based soil moisture signatures, for example, the event rise time, could potentially provide inference about the dominant runoff response type (Araki et al. 2022). In our study, dividing corresponding runoff patterns into similar and different ones under analogous soil moisture provided insights into the recurrence of runoff patterns and their hydro-meteorological drivers. However, our approach also has limitations. Since the pattern search was based on depthweighted mean soil moisture, with the largest weight assigned to the deep soil layer, short-term dynamics in the topsoil may have been improperly accounted for. Furthermore, to obtain more robust thresholds for determining the similarity of soil moisture patterns, further catchments with a broad range of soil types should be considered. The sensitivity analysis related to the similarity criteria showed that results were most stable in the agricultural catchment, followed by the grassland and forest catchment, respectively (Supporting Information S1). As we conducted our study in three small-scale headwater catchments located in Central Europe, it remains uncertain whether our findings are transferable to more heterogeneous catchments with differing characteristics. Therefore, the time series-based pattern search could also be expanded to other catchments with a large variety of physical and climatic conditions where soil moisture data is available to evaluate influencing factors on event runoff characteristics. In this way, the method may be used to distinguish between runoff processes dominating in groups of similar and different runoff patterns based on a large sample of catchments.

6 | Summary and Conclusions

We detected repeating temporal patterns in soil moisture and analysed the influence of hydro-meteorological variables on the corresponding runoff characteristics. Repeating soil moisture patterns occurred in all three catchments, with more groups of patterns formed in the forest and agricultural catchments compared to the grassland catchment. Splitting respective runoff patterns into similar and different, we found that while the wetness-derived variables of ASM and groundwater levels were significantly correlated with event characteristics for similar runoff patterns, correlation coefficients mainly decreased for different runoff patterns in the forest and grassland catchments. Our results, therefore, demonstrated that wetnessderived variables were likely decisive for generating a similar runoff response during analogous soil moisture conditions in two of the three catchments tested. In the forest catchment, the strong influence of soil moisture and groundwater levels implied a fast pressure response between the wetness-derived variables and the stream. In the grassland catchment, the dominant role of soil moisture in the topsoil suggested a substantial contribution of interflow to the stream. In the agricultural catchment, runoff characteristics of similar runoff patterns showed a strong correlation with rainfall-derived variables in addition to soil moisture. Furthermore, rainfall characteristics impacted the normalised peak runoff, irrespective of the shape of the observed hydrograph. Together with the observed earlier peak of the hydrograph compared to soil moisture for identified patterns, our results emphasise the importance of overland flow processes in the catchment.

The time series-based pattern search thus provides a novel framework for analysing runoff characteristics and their drivers, helping to evaluate the dominant hydrological processes in small-scale catchments. Extending the proposed approach to a large sample of catchments has the potential to improve our understanding of the recurrence and thus the possible predictability of runoff patterns and their drivers.

Acknowledgements

This work was funded by the Austrian Science Fund (FWF—Österreichischer Wissenschaftsfonds) (grant number 10.55776/P34666). We acknowledge the support by TERENO (Terrestrial Environmental Observatories) of the Helmholtz Association of National Research Centers (HGF), Germany. The work of Adriane Hövel was supported by the Doctoral School 'Human River Systems in the 21st Century (HR21)' of the BOKU University, Vienna. We also thank the Austrian Federal Agency for Water Management for providing the data for the Petzenkirchen catchment. Open access funding provided by Universitat fur Bodenkultur Wien/KEMÖ.

Conflicts of Interest

The authors declare no conflicts of interest.

Data Availability Statement

The time-series data necessary to reproduce the findings of the study are available in the following data repository: https://doi.org/10.5281/zenodo.13753239 (Hövel et al. 2024b). Furthermore, the tool for the runoff event identification (Giani et al. 2022) used in this paper is available at https://github.com/giuliagiani/DMCA-ESR. The stumpy library

(Python), including the Matrix Profile algorithm (Yeh et al. 2016), used for the time series-based pattern search, can be accessed under https://stumpy.readthedocs.io/en/latest/install.html.

References

- Alaoui, A., U. Caduff, H. H. Gerke, and R. Weingartner. 2011. "Preferential Flow Effects on Infiltration and Runoff in Grassland and Forest Soils." *Vadose Zone Journal* 10, no. 1: 367–377. https://doi.org/10.2136/vzj2010.0076.
- Ali, G., A. Roy, M. C. Turmel, and F. Courchesne. 2010. "Multivariate Analysis as a Tool to Infer Hydrologic Response Types and Controlling Variables in a Humid Temperate Catchment." *Hydrological Processes* 24, no. 20: 2912–2923. https://doi.org/10.1002/hyp.7705.
- Andréassian, V. 2004. "Waters and Forests: From Historical Controversy to Scientific Debate." *Journal of Hydrology* 291, no. 1–2: 1–27. https://doi.org/10.1016/j.jhydrol.2003.12.015.
- Araki, R., F. Branger, I. Wiekenkamp, and H. McMillan. 2022. "A Signature-Based Approach to Quantify Soil Moisture Dynamics Under Contrasting Land-Uses." *Hydrological Processes* 36, no. 4: 1–21. https://doi.org/10.1002/hyp.14553.
- Beiter, D., M. Weiler, and T. Blume. 2020. "Characterising Hillslope–Stream Connectivity With a Joint Event Analysis of Stream and Groundwater Levels." *Hydrology and Earth System Sciences* 24, no. 12: 5713–5744. https://doi.org/10.5194/hess-24-5713-2020.
- Berghuijs, W. R., R. A. Woods, C. J. Hutton, and M. Sivapalan. 2016. "Dominant Flood Generating Mechanisms Across the United States." *Geophysical Research Letters* 43, no. 9: 4382–4390. https://doi.org/10.1002/2016GL068070.
- Blöschl, G. 2006. "Hydrologic Synthesis: Across Processes, Places, and Scales." *Water Resources Research* 42, no. 3: 2–4. https://doi.org/10.1029/2005WR004319.
- Blöschl, G., A. P. Blaschke, M. Broer, et al. 2016. "The Hydrological Open Air Laboratory (HOAL) in Petzenkirchen: A Hypothesis-Driven Observatory." *Hydrology and Earth System Sciences* 20, no. 1: 227–255. https://doi.org/10.5194/hess-20-227-2016.
- Blöschl, G., M. Sivapalan, T. Wagener, A. Viglione, and H. Savenije. 2013. *Runoff Prediction in Ungauged Basins—Synthesis Across Processes, Places and Scales.* Cambridge University Press.
- Blume, T., E. Zehe, and A. Bronstert. 2007. "Rainfall-Runoff Response, Event-Based Runoff Coefficients and Hydrograph Separation." *Hydrological Sciences Journal* 52, no. 5: 843–862. https://doi.org/10.1623/hysj.52.5.843.
- Bogena, H. R., R. Bol, N. Borchard, et al. 2015. "A Terrestrial Observatory Approach to the Integrated Investigation of the Effects of Deforestation on Water, Energy, and Matter Fluxes." *Science China Earth Sciences* 58, no. 1: 61–75. https://doi.org/10.1007/s11430-014-4911-7.
- Bogena, H. R., M. Herbst, J. A. Huisman, U. Rosenbaum, A. Weuthen, and H. Vereecken. 2010. "Potential of Wireless Sensor Networks for Measuring Soil Water Content Variability." *Vadose Zone Journal* 9, no. 4: 1002–1013. https://doi.org/10.2136/vzj2009.0173.
- Bogena, H. R., J. A. Huisman, B. Schilling, A. Weuthen, and H. Vereecken. 2017. "Effective Calibration of Low-Cost Soil Water Content Sensors." *Sensors* 17, no. 1: 208. https://doi.org/10.3390/s17010208.
- Bogena, H. R., C. Montzka, J. A. Huisman, et al. 2018. "The TERENO-Rur Hydrological Observatory: A Multiscale Multi-Compartment Research Platform for the Advancement of Hydrological Science." *Vadose Zone Journal* 17, no. 1: 1–22. https://doi.org/10.2136/vzj2018.03.0055.
- Borchardt, H. 2012. Einfluss periglazialer Deckschichten auf Abflusssteuerung am Beispiel des anthropogen überprägten Wüstebaches. Rheinisch-Westfälische Technische Hochschule Aachen.

- Brocca, L., T. Tullo, F. Melone, T. Moramarco, and R. Morbidelli. 2012. "Catchment Scale Soil Moisture Spatial-Temporal Variability." *Journal of Hydrology* 422: 63–75. https://doi.org/10.1016/j.jhydrol.2011.12.039.
- Brutsaert, W., and J. L. Nieber. 1977. "Regionalized Drought Flow Hydrographs From a Mature Glaciated Plateau." *Water Resources Research* 13, no. 3: 637–643.
- Chen, X., J. Parajka, B. Széles, P. Strauss, and G. Blöschl. 2020a. "Controls on Event Runoff Coefficients and Recession Coefficients for Different Runoff Generation Mechanisms Identified by Three Regression Methods." *Journal of Hydrology and Hydromechanics* 68, no. 2: 155–169. https://doi.org/10.2478/johh-2020-0008.
- Chen, X., J. Parajka, B. Széles, P. Strauss, and G. Blöschl. 2020b. "Spatial and Temporal Variability of Event Runoff Characteristics in a Small Agricultural Catchment." *Hydrological Sciences Journal* 65, no. 13: 2185–2195. https://doi.org/10.1080/02626667.2020.1798451.
- Detty, J. M., and K. J. McGuire. 2010. "Threshold Changes in Storm Runoff Generation at a Till-Mantled Headwater Catchment." *Water Resources Research* 46, no. 7: 1–15. https://doi.org/10.1029/2009WR008102.
- Dralle, D. N., N. Karst, K. Charalampous, A. Veenstra, and S. E. Thompson. 2017. "Event-Scale Power Law Recession Analysis: Quantifying Methodological Uncertainty." *Hydrology and Earth System Sciences* 21, no. 1: 65–81. https://doi.org/10.5194/hess-21-65-2017.
- Dralle, D. N., N. Karst, and S. E. Thompson. 2015. "a, b Careful: The Challenge of Scale Invariance for Comparative Analyses in Power Law Models of the Streamflow Recession." *Geophysical Research Letters* 42, no. 21: 9285–9293. https://doi.org/10.1002/2015GL066007.
- Eder, A., G. Weigelhofer, M. Pucher, et al. 2022. "Pathways and Composition of Dissolved Organic Carbon in a Small Agricultural Catchment During Base Flow Conditions." *Ecohydrology and Hydrobiology* 22, no. 1: 96–112. https://doi.org/10.1016/j.ecohyd.2021. 07.012.
- Exner-Kittridge, M., P. Strauss, G. Blöschl, A. Eder, E. Saracevic, and M. Zessner. 2016. "The Seasonal Dynamics of the Stream Sources and Input Flow Paths of Water and Nitrogen of an Austrian Headwater Agricultural Catchment." *Science of the Total Environment* 542: 935–945. https://doi.org/10.1016/j.scitotenv.2015.10.151.
- Gaál, L., J. Szolgay, T. Bacigál, et al. 2016. "Similarity of Empirical Copulas of Flood Peak-Volume Relationships: A Regional Case Study of North-West Austria." *Contributions to Geophysics & Geodesy* 46, no. 3: 155–178. https://doi.org/10.1515/congeo-2016-0011.
- Gaál, L., J. Szolgay, S. Kohnová, et al. 2015. "Dependence Between Flood Peaks and Volumes: A Case Study on Climate and Hydrological Controls." *Hydrological Sciences Journal* 60, no. 6: 968–984. https://doi.org/10.1080/02626667.2014.951361.
- Gaál, L., J. Szolgay, S. Kohnová, et al. 2012. "Flood Timescales: Understanding the Interplay of Climate and Catchment Processes Through Comparative Hydrology." *Water Resources Research* 48, no. 4: 1–21. https://doi.org/10.1029/2011WR011509.
- Gebler, S., W. Kurtz, V. R. N. Pauwels, S. J. Kollet, H. Vereecken, and H. J. Hendricks Franssen. 2019. "Assimilation of High-Resolution Soil Moisture Data Into an Integrated Terrestrial Model for a Small-Scale Head-Water Catchment." *Water Resources Research* 55, no. 12: 10358–10385. https://doi.org/10.1029/2018WR024658.
- Giani, G., M. A. Rico-Ramirez, and R. A. Woods. 2021. "A Practical, Objective, and Robust Technique to Directly Estimate Catchment Response Time." *Water Resources Research* 57, no. 2: 1–17. https://doi.org/10.1029/2020WR028201.
- Giani, G., L. Tarasova, R. A. Woods, and M. A. Rico-Ramirez. 2022. "An Objective Time-Series-Analysis Method for Rainfall-Runoff Event Identification." *Water Resources Research* 58, no. 2: 1–18. https://doi.org/10.1029/2021WR031283.

- Graf, A., H. R. Bogena, C. Drüe, et al. 2014. "Spatiotemporal Relations Between Water Budget Components and Soil Water Content in a Forested Tributary Catchment." *Water Resources Research* 50, no. 6: 4837–4857. https://doi.org/10.1002/2013WR014516.
- Grimaldi, C., Z. Thomas, M. Fossey, Y. Fauvel, and P. Merot. 2009. "High Chloride Concentrations in the Soil and Groundwater Under an Oak Hedge in the West of France: An Indicator of Evapotranspiration and Water Movement." *Hydrological Processes* 23: 1865–1873. https://doi.org/10.1002/hyp.7316.
- Guo, D., S. Westra, and H. R. Maier. 2017a. "Impact of Evapotranspiration Process Representation on Runoff Projections From Conceptual Rainfall-Runoff Models." *Water Resources Research* 53, no. 1: 435–454. https://doi.org/10.1002/2016WR019627.
- Guo, D., S. Westra, and H. R. Maier. 2017b. "Use of a Scenario-Neutral Approach to Identify the Key Hydro-Meteorological Attributes That Impact Runoff From a Natural Catchment." *Journal of Hydrology* 554: 317–330. https://doi.org/10.1016/j.jhydrol.2017.09.021.
- Harman, C. J., M. Sivapalan, and P. Kumar. 2009. "Power Law Catchment-Scale Recessions Arising From Heterogeneous Linear Small-Scale Dynamics." *Water Resources Research* 45, no. 9: 1–13. https://doi.org/10.1029/2008WR007392.
- Hornbeck, J. W., M. B. Adams, E. S. Corbett, E. S. Verry, and J. A. Lynch. 1993. "Long-Term Impacts of Forest Treatments on Water Yield: A Summary for Northeastern USA." *Journal of Hydrology* 150, no. 2–4: 323–344. https://doi.org/10.1016/0022-1694(93)90115-P.
- Hövel, A., C. Stumpp, H. Bogena, et al. 2024a. "Repeating Patterns in Runoff Time Series: A Basis for Exploring Hydrologic Similarity of Precipitation and Catchment Wetness Conditions." *Journal of Hydrology* 629: 130585. https://doi.org/10.1016/j.jhydrol.2023.130585.
- Hövel, A., C. Stumpp, H. Bogena, et al. 2024b. "Supplement to "Hydro-Meteorological Drivers of Event Runoff Characteristics Under Analogous Soil Moisture Patterns in Three Small-Scale Headwater Catchments" [Data set]." Zenodo. https://doi.org/10.5281/zenodo. 13753239.
- Hrachowitz, M., H. H. G. Savenije, G. Blöschl, et al. 2013. "A Decade of Predictions in Ungauged Basins (PUB)—A Review." *Hydrological Sciences Journal* 58, no. 6: 1198–1255. https://doi.org/10.1080/02626667. 2013.803183.
- Hrachowitz, M., M. Stockinger, M. Coenders-Gerrits, et al. 2021. "Reduction of Vegetation-Accessible Water Storage Capacity After Deforestation Affects Catchment Travel Time Distributions and Increases Young Water Fractions in a Headwater Catchment." *Hydrology and Earth System Sciences* 25, no. 9: 4887–4915. https://doi.org/10.5194/hess-25-4887-2021.
- James, A. L., and N. T. Roulet. 2007. "Investigating Hydrologic Connectivity and Its Association With Threshold Change in Runoff Response in a Temperate Forested Watershed." *Hydrological Processes* 21: 3391–3408. https://doi.org/10.1002/hyp.6554.
- Jencso, K. G., and B. L. McGlynn. 2011. "Hierarchical Controls on Runoff Generation: Topographically Driven Hydrologic Connectivity, Geology, and Vegetation." *Water Resources Research* 47, no. 11: 1–16. https://doi.org/10.1029/2011WR010666.
- Jencso, K. G., B. L. McGlynn, M. N. Gooseff, S. M. Wondzell, K. E. Bencala, and L. A. Marshall. 2009. "Hydrologic Connectivity Between Landscapes and Streams: Transferring Reach- and Plot-Scale Understanding to the Catchment Scale." Water Resources Research 45, no. 4: 1–16. https://doi.org/10.1029/2008WR007225.
- Kirchner, J. W. 2024. "Characterizing Nonlinear, Nonstationary, and Heterogeneous Hydrologic Behavior Using Ensemble Rainfall-Runoff Analysis (ERRA): Proof of Concept." *Hydrology and Earth System Sciences* 28: 4427–4454. https://doi.org/10.5194/hess-28-4427-2024.
- Korres, W., T. G. Reichenau, P. Fiener, et al. 2015. "Spatio-Temporal Soil Moisture Patterns—A Meta-Analysis Using Plot to Catchment Scale

- Data." Journal of Hydrology 520: 326–341. https://doi.org/10.1016/j.jhydrol.2014.11.042.
- Latron, J., and F. Gallart. 2008. "Runoff Generation Processes in a Small Mediterranean Research Catchment (Vallcebre, Eastern Pyrenees)." *Journal of Hydrology* 358, no. 3–4: 206–220. https://doi.org/10.1016/j.jhydrol.2008.06.014.
- Lee, J. Y., C. J. Yang, T. R. Peng, T. Y. Lee, and J. C. Huang. 2023. "Landscape Structures Regulate the Contrasting Response of Recession Along Rainfall Amounts." *Hydrology and Earth System Sciences* 27, no. 23: 4279–4294. https://doi.org/10.5194/hess-27-4279-2023.
- Li, Y. Y., and M. A. Shao. 2006. "Change of Soil Physical Properties Under Long-Term Natural Vegetation Restoration in the Loess Plateau of China." *Journal of Arid Environments* 64, no. 1: 77–96. https://doi.org/10.1016/j.jaridenv.2005.04.005.
- Lindström, G. 1997. "A Simple Automatic Calibration Routine for the HBV Model." *Hydrology Research* 28, no. 3: 153–168.
- Liu, S., I. Van Meerveld, Y. Zhao, Y. Wang, and J. W. Kirchner. 2024. "Seasonal Dynamics and Spatial Patterns of Soil Moisture in a Loess Catchment." *Hydrology and Earth System Sciences* 28, no. 1: 205–216. https://doi.org/10.5194/hess-28-205-2024.
- Madrid, F., S. Imani, R. Mercer, Z. Zimmerman, N. Shakibay, and E. Keogh. 2019. "Matrix Profile XX: Finding and Visualizing Time Series Motifs of All Lengths Using the Matrix Profile." In *Proceedings—10th IEEE International Conference on Big Knowledge, ICBK 2019*, 175–182. IEEE. https://doi.org/10.1109/ICBK.2019.00031.
- Mälicke, M., S. K. Hassler, T. Blume, M. Weiler, and E. Zehe. 2020. "Soil Moisture: Variable in Space but Redundant in Time." *Hydrology and Earth System Sciences* 24, no. 5: 2633–2653. https://doi.org/10.5194/hess-24-2633-2020.
- Merz, R., and G. Blöschl. 2009. "A Regional Analysis of Event Runoff Coefficients With Respect to Climate and Catchment Characteristics in Austria." *Water Resources Research* 45, no. 1: 1–19. https://doi.org/10.1029/2008WR007163.
- Merz, R., G. Blöschl, and J. Parajka. 2006. "Spatio-Temporal Variability of Event Runoff Coefficients." *Journal of Hydrology* 331, no. 3–4: 591–604. https://doi.org/10.1016/j.jhydrol.2006.06.008.
- Mohanty, B. P., M. H. Cosh, V. Lakshmi, and C. Montzka. 2017. "Soil Moisture Remote Sensing: State-of-the-Science." *Vadose Zone Journal* 16, no. 1: 1–9. https://doi.org/10.2136/vzj2016.10.0105.
- Moriasi, D. N., J. G. Arnold, M. W. van Liew, R. L. Bingner, R. D. Harmel, and T. L. Veith. 2007. "Model Evaluation Guidelines for Systematic Quantification of Accuracy in Watershed Simulations." *Transactions of the ASABE* 50, no. 3: 885–900.
- Parajka, J., G. Blöschl, and R. Merz. 2007. "Regional Calibration of Catchment Models: Potential for Ungauged Catchments." *Water Resources Research* 43, no. 6: 1–16. https://doi.org/10.1029/2006W R005271.
- Pavlin, L., B. Széles, P. Strauss, A. P. Blaschke, and G. Blöschl. 2021. "Event and Seasonal Hydrologic Connectivity Patterns in an Agricultural Headwater Catchment." *Hydrology and Earth System Sciences* 25, no. 4: 2327–2352. https://doi.org/10.5194/hess-25-2327-2021.
- Penna, D., H. J. Tromp-Van Meerveld, A. Gobbi, M. Borga, and G. Dalla Fontana. 2011. "The Influence of Soil Moisture on Threshold Runoff Generation Processes in an Alpine Headwater Catchment." *Hydrology and Earth System Sciences* 15, no. 3: 689–702. https://doi.org/10.5194/hess-15-689-2011.
- Qu, W., H. R. Bogena, J. A. Huisman, et al. 2016. "The Integrated Water Balance and Soil Data Set of the Rollesbroich Hydrological Observatory." *Earth System Science Data* 8, no. 2: 517–529. https://doi.org/10.5194/essd-8-517-2016.
- Qu, W., H. R. Bogena, J. A. Huisman, and H. Vereecken. 2013. "Calibration of a Novel Low-Cost Soil Water Content Sensor Based on

a Ring Oscillator." *Vadose Zone Journal* 12, no. 2: 1–10. https://doi.org/10.2136/vzj2012.0139.

Richter, F. 2008. Bodenkarte zur Standorterkundung. Verfahren Quellgebiet Wüstebachtal (Forst). Geologischer Dienst Nordrhein-Westfalen.

Rosenbaum, U., H. R. Bogena, M. Herbst, et al. 2012. "Seasonal and Event Dynamics of Spatial Soil Moisture Patterns at the Small Catchment Scale." *Water Resources Research* 48, no. 10: 1–22. https://doi.org/10.1029/2011WR011518.

Rossi, M. W., K. X. Whipple, and E. R. Vivoni. 2016. "Precipitation and Evapotranspiration Controls on Daily Runoff Variability." *Journal of Geophysical Research. Earth Surface* 121, no. 1: 128–145. https://doi.org/10.1002/2015JF003446.

Saffarpour, S., A. W. Western, R. Adams, and J. J. McDonnell. 2016. "Multiple Runoff Processes and Multiple Thresholds Control Agricultural Runoff Generation." *Hydrology and Earth System Sciences* 20, no. 11: 4525–4545. https://doi.org/10.5194/hess-20-4525-2016.

Saleh, A., J. G. Arnold, P. W. Gassman, et al. 2000. "Application of SWAT for the Upper North Bosque River Watershed." *Transactions of the American Society of Agricultural Engineers* 43, no. 5: 1077–1087. https://doi.org/10.13031/2013.3000.

Sherman, L. 1932. "Streamflow From Rainfall by the Unit-Graph Method." *Engineering News Records* 108: 501–505.

Singh, J., H. V. Knapp, J. G. Arnold, and M. Demissie. 2005. "Hydrological Modeling of the Iroquois River Watershed Using HSPF and SWAT." *Journal of the American Water Resources Association* 41, no. 2: 343–360. https://doi.org/10.1111/j.1752-1688.2005.tb03740.x.

Singh, N. K., R. E. Emanuel, B. L. McGlynn, and C. F. Miniat. 2021. "Soil Moisture Responses to Rainfall: Implications for Runoff Generation." *Water Resources Research* 57, no. 9: 1–17. https://doi.org/10.1029/2020W R028827.

Stein, L., F. Pianosi, and R. Woods. 2020. "Event-Based Classification for Global Study of River Flood Generating Processes." *Hydrological Processes* 34, no. 7: 1514–1529. https://doi.org/10.1002/hyp.13678.

Stockinger, M., H. R. Bogena, A. Lücke, B. Diekkrüger, M. Weiler, and H. Vereecken. 2014. "Seasonal Soil Moisture Patterns: Controlling Transit Time Distributions in a Forested Headwater Catchment." *Water Resources Research* 50, no. 6: 5270–5289. https://doi.org/10.1002/2013W R014815.

Stockinger, M., H. R. Bogena, A. Lücke, C. Stumpp, and H. Vereecken. 2019. "Time Variability and Uncertainty in the Fraction of Young Water in a Small Headwater Catchment." *Hydrology and Earth System Sciences* 23, no. 10: 4333–4347. https://doi.org/10.5194/hess-23-4333-2019.

Széles, B., M. Broer, J. Parajka, et al. 2018. "Separation of Scales in Transpiration Effects on Low Flows: A Spatial Analysis in the Hydrological Open Air Laboratory." *Water Resources Research* 54, no. 9: 6168–6188. https://doi.org/10.1029/2017WR022037.

Szeles, B., L. Holko, J. Parajka, et al. 2024. "Comparison of Two Isotopic Hydrograph Separation Methods in the Hydrological Open Air Laboratory, Austria." *Hydrological Processes* 38, no. 7: 1–15. https://doi.org/10.1002/hyp.15222.

Tarasova, L., S. Basso, C. Poncelet, and R. Merz. 2018. "Exploring Controls on Rainfall-Runoff Events: 2. Regional Patterns and Spatial Controls of Event Characteristics in Germany." *Water Resources Research* 54, no. 10: 7688–7710. https://doi.org/10.1029/2018WR022588.

Tarasova, L., S. Basso, M. Zink, and R. Merz. 2018. "Exploring Controls on Rainfall-Runoff Events: 1. Time Series-Based Event Separation and Temporal Dynamics of Event Runoff Response in Germany." *Water Resources Research* 54, no. 10: 7711–7732. https://doi.org/10.1029/2018WR022587.

TERENO. 2024. "TERENO Data Discovery Portal—Eifel/Lower Rhine Valley Observatory." https://ddp.tereno.net/ddp/.

VanTromp-Meerveld, H. J., and J. J. McDonnell. 2006. "Threshold Relations in Subsurface Stormflow: 2. The Fill and Spill Hypothesis." *Water Resources Research* 42, no. 2: 1–11. https://doi.org/10.1029/2004W R003800.

Vichta, T., J. Deutscher, O. Hemr, et al. 2024. "Combined Effects of Rainfall-Runoff Events and Antecedent Soil Moisture on Runoff Generation Processes in an Upland Forested Headwater Area." *Hydrological Processes* 38, no. 6: 1–15. https://doi.org/10.1002/hyp. 15216.

Vreugdenhil, M., B. Széles, W. Wagner, et al. 2022. "Non-Linearity in Event Runoff Generation in a Small Agricultural Catchment." *Hydrological Processes* 36, no. 8: 1–16. https://doi.org/10.1002/hyp. 14667

Wiekenkamp, I., J. A. Huisman, H. R. Bogena, et al. 2016a. "Changes in Measured Spatiotemporal Patterns of Hydrological Response After Partial Deforestation in a Headwater Catchment." *Journal of Hydrology* 542: 648–661. https://doi.org/10.1016/j.jhydrol.2016.09.037.

Wiekenkamp, I., J. A. Huisman, H. R. Bogena, H. S. Lin, and H. Vereecken. 2016b. "Spatial and Temporal Occurrence of Preferential Flow in a Forested Headwater Catchment." *Journal of Hydrology* 534: 139–149. https://doi.org/10.1016/j.jhydrol.2015.12.050.

Yao, L., D. A. Libera, M. Kheimi, A. Sankarasubramanian, and D. Wang. 2020. "The Roles of Climate Forcing and Its Variability on Streamflow at Daily, Monthly, Annual, and Long-Term Scales." *Water Resources Research* 55, no. 7: 1–23. https://doi.org/10.1029/2020WR027111.

Yeh, C.-C. M., Y. Zhu, L. Ulanova, et al. 2016. "Matrix Profile I: All Pairs Similarity Joins for Time Series: A Unifying View That Includes Motifs, Discords and Shapelets." In *IEEE 16th International Conference on Data Mining (ICDM)*, 1317–1322. IEEE. https://doi.org/10.1109/icdm. 2016.0179.

Zheng, Y., G. Coxon, R. Woods, J. Li, and P. Feng. 2023. "Controls on the Spatial and Temporal Patterns of Rainfall-Runoff Event Characteristics—A Large Sample of Catchments Across Great Britain." Water Resources Research 59, no. 6: 1–25. https://doi.org/10.1029/2022wr033226.

Supporting Information

Additional supporting information can be found online in the Supporting Information section. $\,$